diagnostics

MDPI

Article

Diagnostic Yield and Genotype–Phenotype Correlation of Prenatal Exome Sequencing in Fetuses with Suspected Skeletal Disorders

Milena Perisic Mitrovic [1], Bojana Petrovic [1,*], Irena Marjanovic [2], Olivera Kontic Vucinic [3], Svetlana Vrzic Petronijevic [3], Tijana Janjic [3] and Marina Andjelkovic [2]

[1] Clinic for Gynecology and Obstetrics, University Clinical Center of Serbia, 11000 Belgrade, Serbia
[2] Institute of Molecular Genetics and Genetic Engineering, University of Belgrade, 11000 Belgrade, Serbia
[3] Faculty of Medicine, University of Belgrade, 11000 Belgrade, Serbia
* Correspondence: mrdrbojaninmail@gmail.com

Abstract

Background: Prenatal diagnosis of fetal skeletal disorders remains challenging because of their marked phenotypic heterogeneity, overlapping ultrasound features, and extensive genetic diversity. While chromosomal microarray analysis (CMA) is recommended as a first-tier genetic test, its diagnostic yield is limited for disorders predominantly caused by single-gene variants. This study evaluated the diagnostic contribution and clinical utility of prenatal trio-based whole-exome sequencing (WES) in fetuses with suspected skeletal disorders following normal CMA results. **Methods:** We retrospectively analyzed 24 fetuses with prenatally suspected skeletal anomalies referred to a tertiary fetal medicine center between 2022 and 2026. All cases underwent detailed prenatal ultrasound assessment, normal first-tier CMA, and trio-based WES. Clinical, molecular, inheritance, and genotype–phenotype correlation analyses were performed. **Results:** Pathogenic or likely pathogenic (P/LP) variants were identified in 15 of 24 fetuses (62.5%), comprising 16 variants across ten genes. A phenotype-concordant molecular diagnosis was established in 11 cases (45.8%). *FGFR3* was the most frequently affected gene, accounting for five cases (20.8%). After excluding *FGFR3*-related cases, phenotype-concordant molecular diagnoses were identified in 6 of the remaining 19 fetuses (31.6%). Three additional P/LP findings involving *OTC*, *COL4A5*, and *GNAS* were considered incidental, while the phenotype–genotype relationship remained uncertain in two cases. No phenotype-explanatory molecular finding was identified in nine fetuses (37.5%). **Conclusions:** Prenatal trio-based WES contributes substantially to the molecular evaluation of fetal skeletal disorders following normal first-tier CMA results. The distinction between P/LP variant detection and phenotype-concordant diagnosis highlights the importance of detailed fetal phenotyping and careful variant interpretation. Integrating ultrasound findings with genomic analysis supports genetic counseling and recurrence-risk assessment, while periodic data reanalysis and complementary genomic approaches may help resolve cases without a molecular diagnosis.

Keywords: prenatal diagnosis; skeletal dysplasia; whole-exome sequencing; fetal ultrasound; chromosomal microarray; FGFR3; genotype–phenotype correlation

Check for updates

Academic Editors: Ye Cao and Wing-Cheong Leung

Received: 17 October 2026
Revised: 16 November 2026
Accepted: 19 November 2026
Published: 21 November 2026

Copyright: © 2026 by the authors. Licensee MDPI, Basel, Switzerland. This article is an open access article distributed under the terms and conditions of the Creative Commons Attribution (CC BY) license.

1. Introduction

Fetal skeletal disorders comprise a relatively common group of congenital anomalies, with an estimated incidence of approximately 3–5 per 1000 pregnancies. They encompass a

broad and heterogeneous spectrum of conditions, including skeletal dysplasias, dysostoses, dysmelia, and secondary skeletal malformations. Skeletal dysplasias are further classified into chondrodysplasias, osteodysplasias, spondylodysplasias, thoracic dysplasias, and dysplasias predominantly affecting the epiphyses or metaphyses [1].

Prenatal diagnosis of fetal skeletal disorders remains particularly challenging because of their marked phenotypic heterogeneity and the substantial overlap in ultrasound findings among different conditions. Prenatal ultrasonography is the primary imaging modality for detecting fetal abnormalities; however, its reported sensitivity for diagnosing skeletal disorders remains approximately 50%, even when examinations are performed according to international guidelines. In addition, most skeletal abnormalities become sonographically apparent only during the late second or early third trimester, further complicating prenatal diagnosis and clinical decision-making [2].

Approximately 70% of fetal skeletal disorders have an underlying genetic etiology, predominantly involving monogenic variants and, less frequently, numerical or structural chromosomal abnormalities [3]. The genetic basis of common skeletal disorders, including achondroplasia and osteogenesis imperfecta, has been well characterized and is most frequently associated with pathogenic variants in the *FGFR3*, *COL1A1*, *COL1A2*, and *COL2A1* genes. However, the genetic mechanisms underlying many less frequently diagnosed prenatal skeletal disorders remain incompletely understood [4].

By 2015, causative genes had been identified for more than 150 skeletal dysplasia entities, primarily through positional cloning approaches [5]. The subsequent implementation of whole-exome sequencing (WES) substantially expanded the understanding and classification of these disorders. Accordingly, the 2019 revision of the Nosology and Classification of Genetic Skeletal Disorders recognized 461 distinct entities associated with 437 disease-causing genes [1,4].

Conventional karyotyping has demonstrated a relatively low diagnostic yield (13–16%) in fetuses with sonographically detected short long bones, whereas chromosomal microarray analysis (CMA) provides an additional diagnostic yield ranging from 6% to 27% [6–8]. Because most skeletal disorders result from single-gene variants, the introduction of exome sequencing has markedly improved the molecular diagnosis of these conditions.

Clinical exome sequencing (CES) analyzes approximately 5000 clinically relevant protein-coding genes, whereas WES evaluates approximately 20,000 protein-coding genes. WES primarily enables the detection of single-nucleotide variants (SNVs) and small insertions/deletions (indels) and, depending on the analytical pipeline, may also detect copy number variants (CNVs) [9]. Recent studies suggest that WES should be considered when a specific skeletal disorder is suspected or when femur length measures more than four standard deviations below the mean [7,10].

Despite its high diagnostic yield, the widespread implementation of next-generation sequencing in prenatal diagnosis remains limited by its cost and technical complexity. Consequently, its full potential has not yet been realized in routine clinical practice. The present study aimed to evaluate the diagnostic yield of prenatal WES and genotype–phenotype correlations in fetuses with suspected skeletal disorders, thereby contributing to more accurate prenatal diagnosis, genetic counseling, and clinical management.

2. Materials and Methods

2.1. Study Design and Patient Cohort

This was a single-center retrospective study conducted at a tertiary referral institution (University Clinical Center of Serbia). A total of 1380 samples corresponding to 460 fetuses with diverse congenital anomalies and their parents who had undergone trio-based exome sequencing (ES) were included in the study.

Among these, a cohort of 72 samples representing 24 fetuses with prenatally suspected skeletal abnormalities and their parents was included in the present study. Fetuses with congenital anomalies that did not involve the skeletal system were not considered for this analysis. In addition, among cases presenting with suspected fetal skeletal abnormalities, two cases were excluded due to pathogenic first-tier CMA results, while three cases were excluded because the parents declined further invasive prenatal diagnostic testing. Thus, the final study cohort comprised 24 fetuses with prenatally suspected skeletal abnormalities and normal CMA results, together with their parental samples (Figure 1). Prenatal ultrasound findings suggestive of skeletal dysplasia or related skeletal anomalies served as the primary indication for genetic testing.

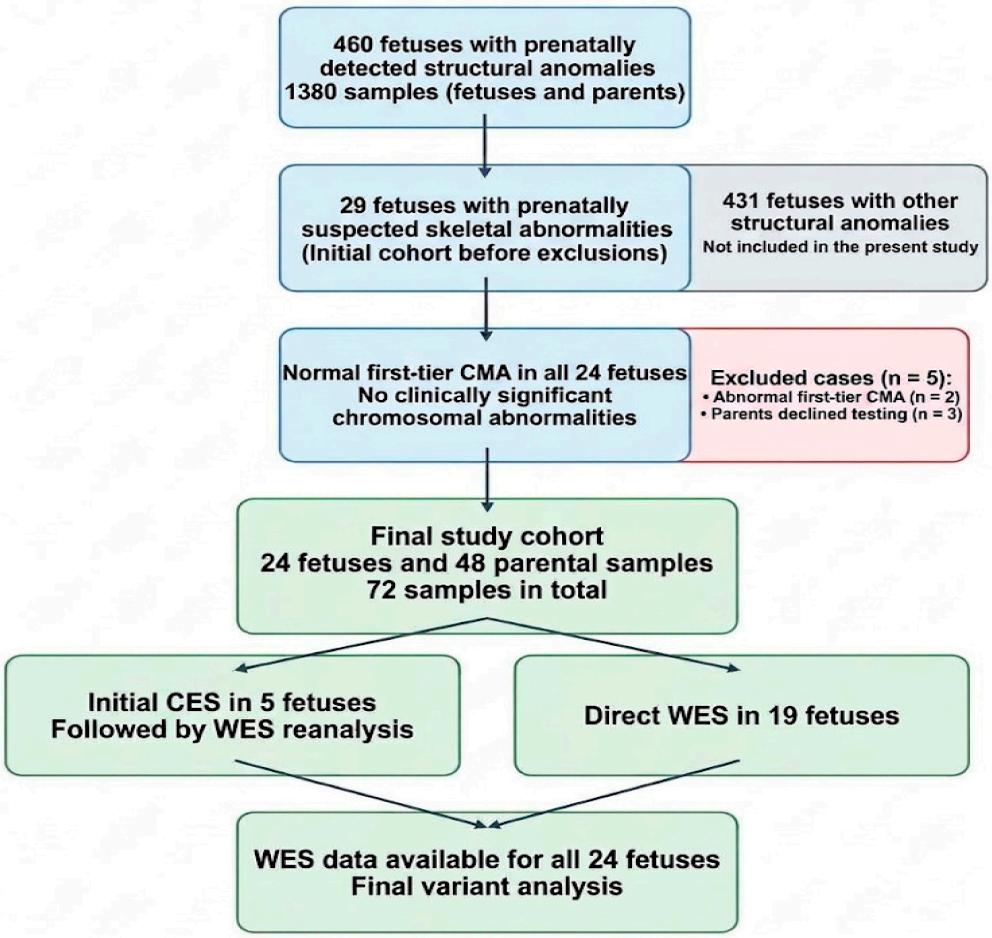


Figure 1. Flowchart of patient selection and study design. A total of 460 fetuses with structural anomalies who underwent trio-based WES were screened. Non-skeletal anomalies, cases with abnormal first-tier CMA results ($n = 2$), and cases where parents declined testing ($n = 3$) were excluded, yielding a final cohort of 24 fetuses with suspected skeletal abnormalities and normal CMA results.

Following detailed fetal ultrasonographic evaluation and multidisciplinary consultation by the Board for Fetal Anomalies, all couples received comprehensive pre- and post-test genetic counseling. Amniocentesis was performed after 16 weeks of gestation upon obtaining written informed consent. Decisions regarding pregnancy management, including termination of pregnancy, were made following multidisciplinary counseling in accordance with institutional regulations. Fetal autopsy and pathological examinations were performed when permitted and available.

2.2. Ethical Approval

The study protocol was approved by the Ethics Committee of the University Clinical Center of Serbia. Written informed consent was obtained from all participating parents prior to invasive procedures and genetic analyses. All clinical data and biological samples were anonymized and processed in strict compliance with ethical standards and research regulations.

2.3. Prenatal Ultrasound Assessment

Ultrasonic evaluations were performed using high-resolution ultrasound systems (Voluson E8/E10, GE Healthcare, Chicago, IL, USA) by experienced fetal medicine specialists at the Board for Fetal Anomalies. Targeted skeletal evaluation encompassed comprehensive biometry, systematic measurement of all long bones (femur, tibia, fibula, humerus, radius, and ulna), assessment of bone shape, curvature, and mineral density, hand and foot morphology, as well as amniotic fluid volume estimation and extra-skeletal organ screening.

2.4. Sample Collection and DNA Extraction

Amniotic fluid (20 mL) was harvested via ultrasound-guided amniocentesis after 16 weeks of gestation. Maternal and paternal peripheral blood samples (5 mL) were collected into EDTA tubes. Genomic DNA was isolated from uncultured amniocytes and parental whole blood using the QIAamp DNA Blood Mini Kit (Qiagen, Düsseldorf, Germany) according to the manufacturer's protocol. DNA concentration and purity were quantified using a Qubit 4.0 Fluorometer with the Quant-iT™ PicoGreen™ dsDNA Assay Kit (Thermo Fisher Scientific, Waltham, MA, USA).

2.5. Chromosomal Microarray Analysis

First-tier CMA was carried out using a high-density oligonucleotide array platform (CytoScan HD/750K Array, Thermo Fisher Scientific, Waltham, MA, USA). Data analysis was performed using Chromosome Analysis Suite (ChAS) software. Only cases with normal CMA results (no reportable pathogenic or likely pathogenic copy number imbalances) proceeded to ES.

2.6. Exome Sequencing

Next-generation sequencing (NGS) was performed on genomic DNA extracted from amniotic fluid and parental peripheral blood samples (trio design). Depending on the diagnostic capabilities available during the study period, either trio-based CES or WES was performed.

The first five fetuses included in the study underwent CES using the TruSight One Gene Panel (Illumina, San Diego, CA, USA), reflecting the diagnostic capabilities available at our institution during the initial phase of the study. These five fetuses were subsequently also analyzed by WES. Following the implementation of WES, all subsequently enrolled fetuses were analyzed using the DNA Prep with Exome 2.5 Enrichment protocol (Illumina, San Diego, CA, USA). Clinical exome sequencing achieved a mean target coverage depth of 90×, with 92% of target bases covered at ≥30×, whereas whole-exome sequencing achieved a mean target coverage depth of 73×, with 86% of target bases covered at ≥30×, providing sufficient sequencing quality for reliable variant detection.

CES libraries were prepared using the Illumina DNA Prep with Enrichment workflow and the TruSight One Gene Panel, targeting 4813 disease-associated genes (Illumina, San Diego, CA, USA). WES libraries were prepared using the DNA Prep with Exome 2.5 Enrichment protocol (Illumina, San Diego, CA, USA). Short-read paired-end sequencing (2 × 150 bp) was performed on the Illumina NextSeq 2000 System (Illumina, San

Diego, CA, USA). Sequence reads were aligned to the human reference genome assembly GRCh38/hg38.

Variants passing quality-control filters (quality score > Q20, read depth > 20×, variant allele fraction ≥ 20%, and minor allele fraction < 1% in the Genome Aggregation Database (gnomAD)) were retained for further analysis. Variant annotation and interpretation were performed using ClinVar and VarSome Clinical [11,12].

To ensure that clinically relevant incidental findings were not overlooked, no automated phenotype-driven variant prioritization pipeline was applied. Instead, all variants passing the predefined quality-control criteria were manually reviewed by experienced molecular geneticists and interpreted in the context of the fetal phenotype, inheritance pattern, population databases, computational prediction tools, and the available scientific literature. Human Phenotype Ontology (HPO) terminology, including Abnormal skeletal morphology (HP:0011842), was used solely for phenotype annotation and was not applied as an automated filtering criterion. Variants were classified according to the joint consensus recommendations of the American College of Medical Genetics and Genomics and the Association for Molecular Pathology (ACMG/AMP) guidelines [13,14].

2.7. Data and Statistical Analysis

Clinical, ultrasonographic, molecular, and autopsy data were systematically recorded. Genotype–phenotype correlation was established by evaluating the clinical concordance between detected molecular variants and observed fetal skeletal dysplasias. Variant-level and case-level analyses were executed independently.

Final diagnoses were established by integrating prenatal ultrasound findings, postnatal findings when available, postmortem examination findings when available, and molecular results. Molecular findings were classified according to their concordance with the observed fetal phenotype. Cases with a pathogenic or likely pathogenic variant consistent with the observed phenotype were classified as phenotype-concordant. Cases in which the relationship between the identified variant and the phenotype could not be established with confidence were classified as having an uncertain phenotype relationship. Variants considered unrelated to the fetal skeletal phenotype were classified as incidental findings. Cases without an identified molecular finding explaining the fetal phenotype were classified as unresolved.

Incidental molecular findings unrelated to skeletal dysplasia were noted separately and excluded from skeletal inheritance pattern calculations.

Descriptive statistical analysis was performed using SPSS Statistics (version 26.0, IBM Corp., Armonk, NY, USA). Continuous variables were summarized as mean ± standard deviation (SD) or median with interquartile range (IQR), as appropriate. Categorical variables were presented as absolute counts and percentages. Due to the limited cohort size (N = 24), inferential statistical testing was not conducted.

3. Results

3.1. Study Population Characteristics

A total of 24 fetuses with prenatally suspected skeletal abnormalities and their parents were included in the analysis. The cohort comprised fetuses referred for advanced genetic evaluation following the detection of suspected skeletal abnormalities on prenatal ultrasound.

The median maternal age was 30.2 ± 5.6 years (median, 29.5 years), while the mean paternal age was 34.4 ± 6.4 years (median, 34 years; range, 24–54 years). The mean gestational age at diagnosis was 28.5 weeks (interquartile range [IQR], 23–31 weeks; range, 16–39 weeks). Fetal sex was female in 12 cases, male in 10 cases, and unknown in two cases.

Among the pregnancies with available cfDNA screening results, all had low-risk results. In contrast, two pregnancies had high-risk results for trisomy 21 on combined first-trimester screening. Subsequent quantitative fluorescent polymerase chain reaction (QF-PCR) testing in both cases did not confirm aneuploidy. All 24 fetuses had normal first-tier CMA results.

Pregnancy outcomes included termination of pregnancy in 16 cases (66.7%), intrauterine fetal demise (IUFD) in one case (4.2%), and delivery in four cases (16.7%). The pregnancy outcome was unknown in three cases (12.5%). Among the delivered infants, one was diagnosed postnatally with Stickler syndrome and another with epiphyseal dysplasia with myopia. Birth anthropometric measurements and Apgar scores were available for the infant in Case 13, whereas detailed postnatal information was unavailable for the infant in Case 24, who was delivered outside our institution.

3.2. Chromosomal Microarray Analysis

All 24 fetuses underwent first-tier CMA, which did not identify clinically significant chromosomal abnormalities, including pathogenic copy-number variants, microdeletions, microduplications, or aneuploidies. All cases subsequently underwent ES for further molecular investigation.

The clinical characteristics, prenatal ultrasound findings, and pregnancy outcomes of all 24 fetuses are summarized in Table 1.

Table 1. Prenatal and postnatal phenotypic findings and pregnancy outcomes.

Case	Maternal Age (Years)	Paternal Age (Years)	GA at Diagnosis (Weeks)	Sex	Prenatal Ultrasound Findings	Pregnancy Outcome	Postmortem/Postnatal Findings
1	27	29	36	Male	Shortening of the long bones	TOP	Shortening of all long bones, without brachydactyly. Maternal ciprofloxacin exposure during the first trimester was reported.
2	33	37	30	Male	Short femora and tibiae; polyhydramnios	TOP	No autopsy available. Marked intrafamilial phenotypic variability reported.
3	32	35	28	Female	Shortening of the long bones	IUFD at 35 weeks	IUGR, shortening of all long bones, mild femoral bowing, and infection.
4	30	31	16	Male	Shortening and bowing of the long bones	TOP	Non-short-trunk chondrodysplasia with platyspondyly; described in the autopsy report as thanatophoric dysplasia.
5	29	32	29	Male	Femoral shortening	TOP	No autopsy available.
6	33	37	39	Female	Shortening of the long bones	Delivery	Postnatal diagnosis of Stickler syndrome. The mother, carrying the same variant, had a milder phenotype. Birth weight 3090 g; length 46 cm; head circumference 33 cm; Apgar score 9.

Table 1. *Cont.*

Case	Maternal Age (Years)	Paternal Age (Years)	GA at Diagnosis (Weeks)	Sex	Prenatal Ultrasound Findings	Pregnancy Outcome	Postmortem/Postnatal Findings
7	36	41	23	Female	Shortening of the long bones	TOP	Symmetric IUGR, shortening of all long bones, chondrodysplasia, facial dysmorphism, and single umbilical artery. The specific type of skeletal dysplasia could not be classified.
8	34	38	31	Male	Proximal shortening of the long bones	Unknown	No postmortem or postnatal information available. *COL4A5* finding considered incidental to the fetal skeletal phenotype.
9	26	34	32	Male	Shortening of the long bones	TOP	Symmetric IUGR, shortened long bones, aortic stenosis, and macrocephaly. The findings may be compatible with achondroplasia, but no molecular diagnosis was established.
10	31	39	34	Male	Shortening of the long bones; oligohydramnios	Unknown	Not delivered at our institution. TORCH screening was unremarkable.
11	25	27	24	Female	Fibulae not visualized; left tibial bowing; posterior positioning of the left foot; foot bones not clearly visualized bilaterally	TOP	Bilateral absence of the fibulae; absence of the fourth and fifth toes bilaterally and the third toe on the right; shortening of both tibiae; right tibial bowing; bilateral foot deformities; cutaneous syndactyly of the second and third toes of the left foot. Findings suggestive of early developmental disruption.
12	24	26	24	Female	Acrania	TOP	Symmetric IUGR, acrania, and anencephaly. First twin pregnancy.
13	28	34	29	Female	Bilateral femoral shortening	Delivery	WES and CMA negative. Birth weight 930 g; length 35 cm; head circumference 26 cm; Apgar score 6.
14	40	42	20	Male	Shortening and bowing of the long bones	TOP	Short and bowed long bones; chondrodysplasia with platyspondyly.
15	33	35	25	Female	Left upper-limb anomaly with partial absence of the forearm and hand	TOP	Amputation of the left arm below the elbow, consistent with an early amniotic band sequence.
16	41	37	22	Female	Shortening and deformity of the long bones	TOP	Chondrodysplasia without short trunk, platyspondyly, and markedly shortened and bowed long bones.

Table 1. *Cont.*

Case	Maternal Age (Years)	Paternal Age (Years)	GA at Diagnosis (Weeks)	Sex	Prenatal Ultrasound Findings	Pregnancy Outcome	Postmortem/Postnatal Findings
17	23	24	21	Unknown	Shortening of the long bones	Unknown	Not delivered at our institution; no postnatal or postmortem confirmation available.
18	27	29	30	Male	Shortening of the long bones; suspected renal cortical cysts; dilated calyces; megacisterna magna	TOP	Shortening of all long bones and femoral bowing; thin vertebral bodies; increased intervertebral spaces; shortened epiphyseal growth cartilage zone with chondrocyte columnization.
19	36	54	20	Female	Shortening of the long bones; femoral bowing; pes equinovarus	Delivery	Postnatal diagnosis of epiphyseal dysplasia with myopia. Birth weight 2800 g; length 43 cm; head circumference 34 cm; Apgar score 7.
20	20	32	30	Female	Shortening of the long bones; left pyelectasis	TOP	Shortening of all long bones, humeral bowing, and dilation of the left renal pelvis.
21	38	40	28	Female	Shortening of the long bones; spina bifida; lemon and banana signs	TOP	Rhizomelia, mesomelia, open spina bifida, ventriculomegaly, and cerebellar hypoplasia. *GNAS* finding considered unrelated to the skeletal phenotype.
22	29	30	39	Female	Shortening of the long bones	TOP	Shortening and bowing of all long bones.
23	22	30	21	Male	Shortening and abnormal shape of all long bones; small stomach; polyhydramnios	TOP	Marked shortening of all tubular bones and bowing of the humeri and lower-leg bones.
24	27	33	31	Unknown	Shortening of the long bones	Delivery outside our institution	Pregnancy continued. Both parents were of short stature (maternal height 149 cm). Detailed postnatal information unavailable.

Abbreviations: GA, gestational age; IUGR, intrauterine growth restriction; IUFD, intrauterine fetal demise; TOP, termination of pregnancy; WES, whole-exome sequencing; CMA, chromosomal microarray analysis; TORCH, toxoplasmosis, other infections, rubella, cytomegalovirus, and herpes simplex.

3.3. Overall Molecular Findings and Phenotype Concordance

Pathogenic or likely pathogenic (P/LP) variants were identified in 15 of the 24 fetuses (62.5%). A total of 16 P/LP variants were detected because two variants were identified in one fetus (Case 4). After integration of the molecular findings with the available prenatal ultrasound, postnatal, and postmortem data, a phenotype-concordant molecular diagnosis was established in 11 cases (45.8%).

In two additional cases, the relationship between the identified P/LP variant and the observed fetal phenotype remained uncertain (*IHH* variant in Case 1 and *GHSR* variant in Case 3). In two other cases, the identified variants were considered incidental and unrelated to the skeletal findings (*COL4A5* variant in Case 8 and *GNAS* variant in Case 21). In Case

4, an additional *OTC* variant was identified alongside the phenotype-concordant *FGFR3* variant and was also considered incidental.

In the remaining nine cases, no P/LP variants were identified.

3.4. Distribution of Variants Across Genes

The 16 P/LP variants identified in 15 fetuses involved 10 genes. *FGFR3* was the most frequently affected gene, with variants detected in five fetuses, followed by *COL2A1*, with three variants. The remaining variants involved *MYH3*, *IHH*, *GHSR*, *OTC*, *COL4A5*, *IFITM5*, *GNAS*, and *COL1A2*.

Most variants were heterozygous. The exception was the hemizygous *OTC* variant identified in Case 4. Most variants were missense substitutions, while the *MYH3* variant in Case 2 affected a splice site and the *IFITM5* variant in Case 20 was located in the 5′ untranslated region.

Case 4 carried two P/LP variants: a de novo *FGFR3* variant considered explanatory for the skeletal phenotype and a maternally inherited *OTC* variant considered incidental.

3.5. FGFR3-Related Findings

Five fetuses carried P/LP variants in *FGFR3* (c.742C>T in Cases 4, 14, and 17; c.1138G>A in Cases 5 and 18), all confirmed as *de novo*. Postmortem findings confirmed thanatophoric dysplasia (Cases 4 and 14) and achondroplasia (Cases 5 and 18), while Case 17 lacked postnatal confirmation. Excluding *FGFR3* cases, phenotype-concordant molecular diagnoses were identified in 6 of the remaining 19 fetuses (31.6%).

3.6. Genetic Characteristics of Detected Variants

Variants in genes other than *FGFR3* accounted for six phenotype-concordant cases and two with uncertain phenotype relationships. These involved *COL2A1* (Cases 6, 19, and 23, with postnatal diagnoses of Stickler syndrome and epiphyseal dysplasia with myopia, and intrafamilial variability in Case 6), *IFITM5* (Case 20, osteogenesis imperfecta type V), *COL1A2* (Case 22), and *MYH3* (Case 2, distal arthrogryposis). Phenotype concordance remained uncertain for an *IHH* variant in Case 1 and a *GHSR* variant in Case 3.

The molecular findings and their genotype–phenotype correlations are summarized in Table 2.

Table 2. Molecular findings and variant interpretation.

Case	WES Result	Gene	Variant	Zygosity	Classification	Inheritance	Interpretation
1	P/LP variant identified	*IHH*	c.1016T>A, p.(Val339Glu)	Heterozygous	Likely pathogenic	De novo	PGR-U; brachydactyly not observed at autopsy.
2	P/LP variant identified	*MYH3*	c.-9+1G>A	Heterozygous	Pathogenic	Paternal	Phenotype-concordant; consistent with distal arthrogryposis. Specific subtype not established.
3	P/LP variant identified	*GHSR*	c.709A>T, p.(Arg237Trp)	Heterozygous	Likely pathogenic	Maternal	PGR-U; contribution of a heterozygous variant remains unclear.
4	Two P/LP variants identified	*FGFR3*; *OTC*	*FGFR3*: c.742C>T, p.Arg248Cys; *OTC*: c.959G>A	Heterozygous; hemizygous, respectively	Pathogenic; likely pathogenic, respectively	*FGFR3*: de novo; *OTC*: maternal	*FGFR3*: Thanatophoric dysplasia type 1 (OMIM 187600), explanatory for the skeletal phenotype. *OTC*: incidental finding.

Table 2. *Cont.*

Case	WES Result	Gene	Variant	Zygosity	Classification	Inheritance	Interpretation
5	P/LP variant identified	*FGFR3*	c.1138G>A, p.Gly380Arg	Heterozygous	Pathogenic	De novo	Achondroplasia (OMIM 100800).
6	P/LP variant identified	*COL2A1*	c.962G>T, p.Gly321Val	Heterozygous	Likely pathogenic	Maternal	Stickler syndrome type 1 (OMIM 108300); postnatal diagnosis.
7	WES negative	—	—	—	—	—	NMF-P.
8	P/LP variant identified	*COL4A5*	c.1871G>A, p.Gly624Asp	Hemizygous	Pathogenic	Maternal	Incidental finding; not considered explanatory for the skeletal phenotype.
9	WES negative	—	—	—	—	—	NMF-P.
10	WES negative	—	—	—	—	—	NMF-P.
11	WES negative	—	—	—	—	—	NMF-P.
12	WES negative	—	—	—	—	—	NMF-P.
13	WES negative; CMA negative	—	—	—	—	—	NMF-P.
14	P/LP variant identified	*FGFR3*	c.742C>T, p.Arg248Cys	Heterozygous	Pathogenic	De novo	Thanatophoric dysplasia type 1 (OMIM 187600); skeletal abnormalities confirmed postmortem.
15	WES negative	—	—	—	—	—	NMF-P.
16	WES negative	—	—	—	—	—	NMF-P.
17	P/LP variant identified	*FGFR3*	c.742C>T, p.Arg248Cys	Heterozygous	Pathogenic	De novo	Molecular finding consistent with thanatophoric dysplasia type 1 (OMIM 187600); postnatal/postmortem confirmation unavailable.
18	P/LP variant identified	*FGFR3*	c.1138G>A, p.Gly380Arg	Heterozygous	Pathogenic	De novo	Achondroplasia (OMIM 100800); postmortem findings further characterized the skeletal phenotype.
19	P/LP variant identified	*COL2A1*	c.2710C>T, p.Arg904Cys	Heterozygous	Pathogenic	De novo	Multiple epiphyseal dysplasia with myopia (OMIM 132450); conductive hearing status not documented.
20	P/LP variant identified	*IFITM5*	c.-14C>T	Heterozygous	Pathogenic	De novo	Osteogenesis imperfecta type V (OMIM 610967).
21	P/LP variant identified	*GNAS*	p.Arg336Trp	Heterozygous	Likely pathogenic	De novo	Incidental finding; not considered explanatory for the skeletal phenotype.
22	P/LP variant identified	*COL1A2*	c.3250G>T, p.Gly1084Cys	Heterozygous	Pathogenic	Paternal	*COL1A2*-related skeletal phenotype; specific clinical diagnosis not established.

Table 2. *Cont.*

Case	WES Result	Gene	Variant	Zygosity	Classification	Inheritance	Interpretation
23	P/LP variant identified	*COL2A1*	c.1681G>C, p.Gly561Arg	Heterozygous	Likely pathogenic	De novo	Phenotype-concordant; postmortem findings supported the molecular interpretation. Specific clinical diagnosis not established.
24	WES negative	—	—	—	—	—	NMF-P.

Abbreviations: CMA, chromosomal microarray analysis; NMF-P, no molecular finding explaining the phenotype; P/LP, pathogenic/likely pathogenic; PGR-U, phenotype–genotype relationship uncertain; WES, whole-exome sequencing.

3.7. Inheritance Patterns

Among the 11 cases with phenotype-concordant molecular findings, eight variants were de novo (72.7%) and three were inherited (27.3%).

The de novo variants were identified in *FGFR3* in Cases 4, 5, 14, 17, and 18, in *COL2A1* in Cases 19 and 23, and in *IFITM5* in Case 20. Inherited variants included the paternally inherited *MYH3* variant in Case 2, the maternally inherited *COL2A1* variant in Case 6, and the paternally inherited *COL1A2* variant in Case 22.

3.8. Prenatal Phenotypic Findings

Shortening of the long bones was the predominant prenatal ultrasound finding in the cohort. Additional skeletal findings included bowing of the long bones, disproportionate shortening of individual segments, abnormal limb positioning, and foot deformities.

Several fetuses also presented with extraskeletal findings. These included polyhydramnios, oligohydramnios, renal pelvic or calyceal dilation, suspected renal cortical cysts, megacisterna magna, and findings suggestive of fetal growth restriction. Central nervous system abnormalities were also observed in some cases.

In Case 11, prenatal ultrasound demonstrated non-visualization of the fibulae, curvature of the left tibia, posterior positioning of the left foot, and failure to distinguish the foot bones bilaterally. In Case 12, the principal prenatal finding was acrania. Case 15 presented with a left upper-limb reduction anomaly, with partial absence of the forearm and hand.

3.9. Genotype–Phenotype and Prenatal–Postmortem Correlation

Postmortem examination provided additional phenotypic information in several cases and enabled comparison with the prenatal ultrasound findings. Among the *FGFR3*-positive cases, postmortem findings in Cases 4 and 14 demonstrated skeletal abnormalities, including platyspondyly and shortening or bowing of the long bones; representative imaging findings for Case 4 are provided in the Supplementary Material (Figure S1). In Case 18, postmortem examination further characterized the skeletal phenotype, revealing abnormalities of the vertebral bodies, intervertebral spaces, and epiphyseal growth cartilage, with representative imaging findings included in the Supplementary Material (Figure S2). In Case 5, postmortem examination was unavailable.

In Case 1, postmortem examination confirmed shortening of all long bones but did not demonstrate brachydactyly, leaving the relationship between the *IHH* variant and the fetal phenotype uncertain.

Among the WES-negative cases, postmortem examination also revealed a range of skeletal and non-skeletal abnormalities. Case 7 showed symmetric intrauterine growth restriction, shortening of all long bones, chondrodysplasia, and facial dysmorphism, although

the specific type of skeletal dysplasia could not be established. Case 9 showed symmetric growth restriction, shortened long bones, aortic stenosis, and macrocephaly. In Case 15, postmortem whole-body radiography further confirmed the left upper-limb anomaly with partial absence of the forearm and hand (amputation below the elbow), consistent with amniotic band sequence. Case 16 demonstrated chondrodysplasia without short trunk, platyspondyly, and markedly shortened and bowed long bones.

In Cases 20, 22, and 23, postmortem findings were consistent with and further characterized the skeletal abnormalities identified prenatally, supporting the interpretation of the corresponding molecular findings. Representative prenatal ultrasound and postmortem radiographic findings of selected cases with positive WES results (Cases 20 and 22) are illustrated in Figures 2 and 3, respectively.

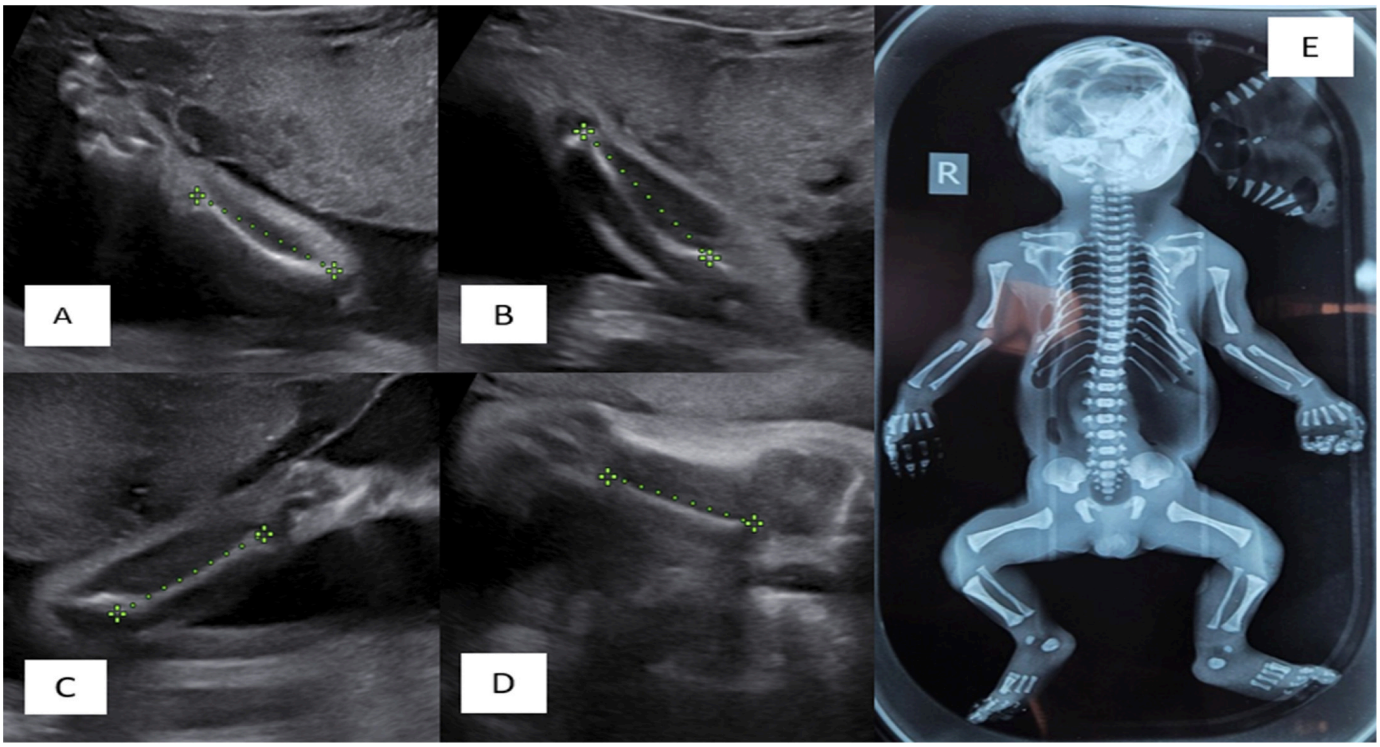


Figure 2. Case 20 (OI type V): Multimodal imaging and genetic findings for the first case: (**A**–**D**) Second-trimester prenatal transabdominal ultrasound scans showing marked and progressive shortening of the upper and lower limb long bones (humerus, radius, ulna, tibia, fibula) alongside detailed foot biometry and low percentiles. (**E**) Postmortem whole-body radiograph (X-ray) demonstrating generalized skeletal involvement, severe limb shortening, and characteristic humeral bowing. Genetic confirmation demonstrating the *IFITM5* variant associated with osteogenesis imperfecta type V.

Furthermore, prenatal ultrasound and postmortem images of selected WES-negative cases (including Cases 7, 9, 15 and 16) demonstrating complex skeletal and structural anomalies are presented in Figures 4, 5, 6 and 7, respectively.

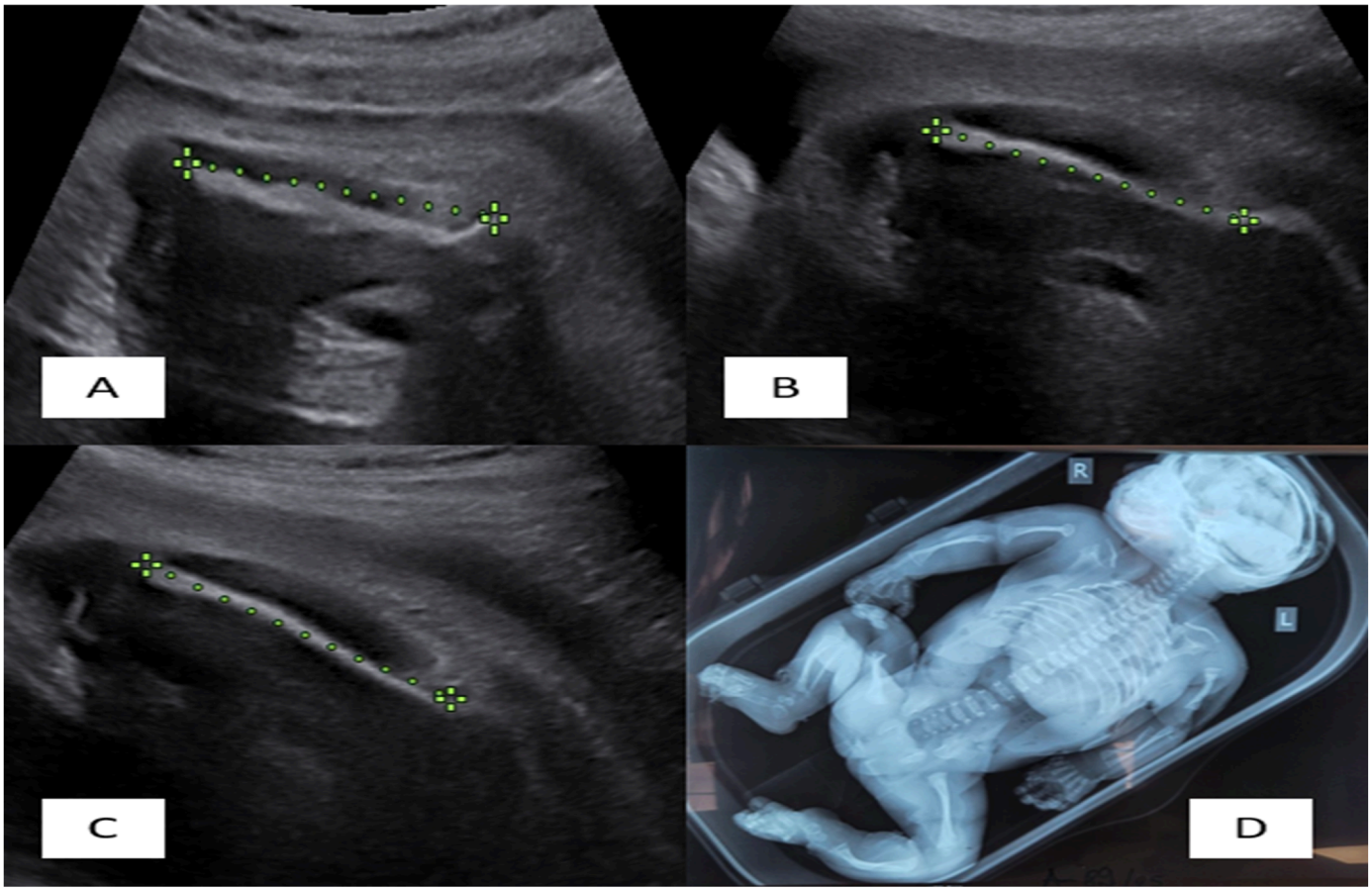


Figure 3. Case 22 (*COL1A2*-related skeletal phenotype): Multimodal imaging findings and genetic profile for the fourth case (*COL1A2*-related skeletal phenotype): (**A**–**C**) Serial third-trimester transabdominal ultrasound scans demonstrating marked shortening and bowing of all long bones; (**D**) Postmortem whole-body radiograph confirming generalized skeletal involvement corresponding to the identified heterozygous pathogenic *COL1A2* variant (c.3250G>T, p.Gly1084Cys).



Figure 4. Case 7 (unclassified skeletal dysplasia, WES-negative): Postmortem whole-body radiograph demonstrating marked generalized shortening of all long bones and chondrodysplasia, corresponding to an unclassified skeletal phenotype with an unremarkable molecular profile (negative WES).

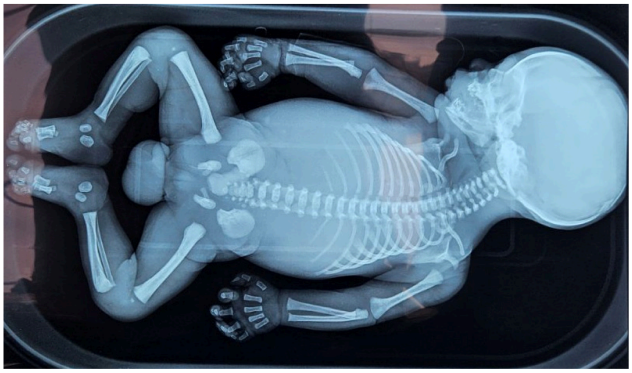


Figure 5. Case 9 (suspected achondroplasia, molecularly unconfirmed): Postmortem whole-body radiograph demonstrating symmetric intrauterine growth restriction, generalized shortening of all long bones, and macrocephaly, consistent with findings potentially compatible with achondroplasia despite the absence of an established molecular diagnosis (negative WES).

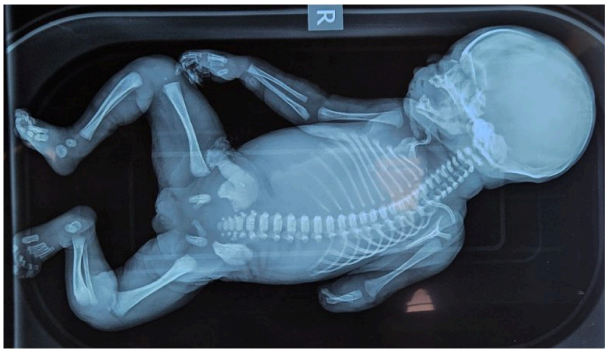


Figure 6. Case 15 (amniotic band sequence): Postmortem whole-body radiograph demonstrating left upper-limb anomaly with partial absence of the forearm and hand (amputation below the elbow), consistent with an early amniotic band sequence (negative WES).



Figure 7. Case 16 (chondrodysplasia without short trunk): Postmortem whole-body radiograph demonstrating platyspondyly and markedly shortened and bowed long bones, consistent with chondrodysplasia without short trunk (negative WES).

3.10. Incidental Molecular Findings

Three P/LP findings were considered incidental and unrelated to the observed skeletal phenotype.

In Case 4, a maternally inherited hemizygous *OTC* c.959G>A variant was identified alongside the phenotype-concordant *FGFR3* variant. In Case 8, a maternally inherited *COL4A5* c.1871G>A (p.Gly624Asp) variant was detected in a male fetus referred because of proximal shortening of the long bones. The variant was not considered explanatory for the skeletal findings. In Case 21, a de novo *GNAS* p.Arg336Trp variant was identified; however, *GNAS* was not considered an explanation for the observed skeletal phenotype.

3.11. WES-Negative Cases and Unresolved Phenotypes

No molecular finding explaining the fetal phenotype was identified in nine cases. These included fetuses with isolated or generalized shortening of the long bones, complex skeletal abnormalities, and non-skeletal structural anomalies.

Case 7 presented with shortened long bones and, at postmortem examination, symmetric intrauterine growth restriction, chondrodysplasia, and facial dysmorphism. Case 9 showed shortened long bones, with postmortem findings of symmetric growth restriction, aortic stenosis, and macrocephaly. Although the phenotype raised the possibility of a skeletal dysplasia, no causative molecular finding was identified. Case 10 presented with shortened long bones and oligohydramnios; the fetus was not delivered at our center, and further postnatal phenotypic information was unavailable.

Case 11 had a complex limb abnormality characterized by bilateral absence of the fibulae, shortening and bowing of the tibiae, foot deformities, and missing toes. Postmortem examination also identified cutaneous syndactyly. The findings were suggestive of an early developmental disruption rather than a defined primary skeletal dysplasia.

Case 12 presented with acrania on prenatal ultrasound, with postmortem confirmation of acrania/anencephaly and symmetric intrauterine growth restriction. Case 13 had bilateral femoral shortening, but both WES and CMA were negative. Birth anthropometric measurements and an Apgar score were recorded. Case 15 presented with a left upper-limb reduction anomaly; postmortem examination demonstrated amputation below the elbow, with findings consistent with an early amniotic band sequence.

Case 16 showed shortening and deformity of the long bones prenatally. Postmortem examination revealed chondrodysplasia without short trunk, platyspondyly, and markedly shortened and bowed long bones, but no causative molecular finding was identified. Finally, Case 24 presented with shortened long bones on prenatal ultrasound. Both parents were of short stature; however, the pregnancy was continued and delivery took place outside our institution. Detailed postnatal phenotypic information was unavailable.

4. Discussion

Prenatal WES identified pathogenic or likely pathogenic (P/LP) variants in 15 of 24 fetuses (62.5%) in our cohort of fetuses with suspected skeletal disorders, comprising 16 variants across ten genes. A phenotype-concordant molecular diagnosis was established in 11 cases (45.8%), supporting the value of WES as a complementary diagnostic tool in pregnancies with sonographically detected skeletal anomalies. The clinical utility of WES is further underscored by the fact that all fetuses included in this study had previously received normal CMA results. Although all fetuses had normal CMA results, two pregnancies had increased risk estimates for trisomy 21 on double screening; both had normal QF-PCR results. Although CMA provides an incremental diagnostic yield of 6–27% in fetuses with structural anomalies, its diagnostic performance remains limited in skeletal dysplasias, which are predominantly caused by single-gene variants and small insertions/deletions rather than chromosomal abnormalities [15,16].

The diagnostic yield observed in our cohort is consistent with previously published studies reporting detection rates ranging from 32.7% to 64% for prenatal exome sequencing in fetuses with suspected skeletal dysplasias following a non-diagnostic chromosomal microarray analysis [17–19]. The phenotype-concordant variants involved genes with essential roles in endochondral ossification, extracellular matrix formation, collagen biosynthesis, and skeletal development, including *FGFR3*, *COL2A1*, *COL1A2*, *IHH*, *MYH3*, and *IFITM5*. Additional P/LP variants were identified in *GHSR*, *OTC*, *COL4A5*, and *GNAS*, although their contribution to the observed skeletal phenotypes was uncertain or considered incidental. This broad molecular spectrum reflects the marked genetic heterogeneity underlying fetal

skeletal disorders and explains the considerable phenotypic overlap frequently encountered during prenatal ultrasound evaluation.

Shortening of the long bones was the predominant prenatal ultrasound finding in our cohort and was frequently accompanied by bowing of long bones, extremity deformities, or extra-skeletal abnormalities such as polyhydramnios and renal abnormalities. Despite these characteristic findings, similar prenatal phenotypes were associated with distinct molecular findings, illustrating the limited specificity of prenatal imaging alone. These observations further support the integration of detailed fetal phenotyping with comprehensive genomic analysis to improve diagnostic accuracy and facilitate appropriate prenatal counseling.

Consistent with previous reports, *FGFR3* was the most frequently affected gene in our cohort, accounting for 20.8% of all cases. Pathogenic *FGFR3* variants are well recognized as the principal molecular cause of thanatophoric dysplasia and achondroplasia, which represent the most common prenatally diagnosed monogenic skeletal dysplasias [18,19]. Variants in *COL2A1* were identified in three fetuses, whereas P/LP variants involving *COL1A2*, *IHH*, *MYH3*, *IFITM5*, and *GHSR* were each detected in one fetus, further emphasizing the molecular diversity of these disorders.

Advanced paternal age has been associated with an increased risk of de novo pathogenic variants in *FGFR3*, particularly those underlying achondroplasia. This association is attributed, at least in part, to age-related clonal expansion of spermatogonial stem cells carrying activating *FGFR3* mutations [20]. In our cohort, paternal age in the five cases with *FGFR3*-related skeletal abnormalities ranged from 24 to 42 years (median, 31 years). Although one father was older than 40 years, the relatively young paternal ages in the remaining cases indicate that advanced paternal age was not a consistent feature of this small subgroup. Nevertheless, these findings do not exclude a potential contribution of paternal age to the occurrence of de novo *FGFR3* variants, as the relationship between paternal age and mutation transmission may differ depending on the specific variant.

Although *FGFR3* accounted for five of the 11 phenotype-concordant molecular diagnoses in our cohort, six additional diagnoses involved other genes. Thus, excluding cases with *FGFR3* variants, phenotype-concordant molecular diagnoses were identified in 31.6% of the remaining cases (6/19). This finding highlights the contribution of exome sequencing beyond the identification of *FGFR3* variants and demonstrates the molecular diversity of prenatal skeletal disorders.

The *IHH* variant identified in Case 1 deserves particular attention. Although pathogenic *IHH* variants are classically associated with autosomal dominant brachydactyly type A1, accumulating evidence indicates that the phenotypic spectrum is considerably broader. Vasques et al. demonstrated that pathogenic *IHH* variants may present predominantly with short stature and isolated long bone shortening in the absence of the characteristic brachydactyly phenotype [21]. However, in our case, the absence of brachydactyly and the additional clinical context mean that the relationship between the identified *IHH* variant and the observed fetal phenotype remains uncertain.

Incidental molecular findings unrelated to the prenatal skeletal phenotype were identified in three cases, involving *OTC*, *COL4A5*, and *GNAS*. These variants are clinically relevant because they are associated with ornithine transcarbamylase deficiency, X-linked Alport syndrome, and *GNAS*-related disorders, respectively. However, none was considered explanatory for the fetal skeletal abnormalities observed in the corresponding pregnancies [22,23]. Their identification nevertheless illustrates one of the important challenges associated with prenatal exome sequencing, namely the detection and appropriate management of secondary or incidental findings. These findings were therefore not considered causative of the skeletal phenotype when assessing genotype–phenotype concordance.

Among the 11 cases with phenotype-concordant molecular findings, eight variants were de novo and three were inherited from a parent. The inherited variants involved *MYH3, COL2A1*, and *COL1A2*. In Case 2, the pathogenic splice-site variant in *MYH3* was inherited from the father, illustrating the potential for intrafamilial phenotypic variability, as previously reported by Kimber et al. [24]. In Case 6, the *COL2A1* variant was inherited from the mother, who had a milder phenotype than the affected child. In Case 22, the *COL1A2* variant was inherited from the father. In addition, the *GHSR* variant in Case 3 was maternally inherited, although its relationship with the fetal phenotype remained uncertain. These findings underscore the complexity of prenatal variant interpretation and demonstrate that inheritance patterns alone cannot reliably predict fetal disease severity. Penetrance and expressivity may vary considerably, making detailed fetal phenotyping, family history, and multidisciplinary genetic counseling essential for accurate interpretation. Although molecular diagnosis substantially improves diagnostic precision, careful clinical correlation remains indispensable for prenatal interpretation and counseling [25].

Comprehensive genetic counseling is therefore fundamental for establishing inheritance patterns and estimating recurrence risks, which may reach 25% or 50% depending on the underlying mode of inheritance [16]. Counseling is optimally delivered within a multidisciplinary team including maternal-fetal medicine specialists, clinical geneticists, and pediatric pathologists. For families carrying inherited pathogenic variants, preimplantation genetic testing (PGT) combined with in vitro fertilization (IVF) may provide a reproductive option for future pregnancies.

Despite the diagnostic contribution of prenatal exome sequencing, no phenotype-concordant molecular finding was identified in nine of the 24 fetuses (37.5%). These unresolved cases highlight the inherent limitations of exome sequencing, which generally does not detect deep intronic variants, regulatory alterations, repeat expansions, balanced structural rearrangements, or certain classes of copy number variation. Moreover, non-genetic mechanisms, including vascular disruption, amniotic band sequence, and teratogenic exposure, should also be considered in the differential diagnosis of prenatally detected skeletal abnormalities.

To improve the diagnostic yield in unresolved cases, periodic reanalysis of exome sequencing data should be considered as novel disease-associated genes and improved variant annotation continue to emerge. Furthermore, for fetuses with persistent clinical suspicion of an underlying genetic disorder despite negative exome sequencing, complementary genomic approaches such as whole-genome sequencing may help identify pathogenic non-coding variants and structural alterations, whereas RNA sequencing may reveal aberrant splicing or other transcript-level abnormalities, in alignment with current ACMG and ISPD prenatal guidelines [26,27].

Several limitations should be acknowledged. The relatively small sample size and retrospective single-center design may have introduced selection bias toward severe phenotypes referred to a tertiary fetal medicine center. In addition, postmortem examination was unavailable in a subset of terminated pregnancies, limiting complete phenotype confirmation, while long-term clinical follow-up was available for only a limited number of cases. Finally, functional validation studies were not performed, and variant interpretation therefore relied on ACMG/AMP classification criteria supported by bioinformatic prediction tools and publicly available variant databases.

Despite these limitations, our findings demonstrate that prenatal exome sequencing contributes substantially to the molecular evaluation of fetal skeletal disorders when integrated with detailed prenatal ultrasound assessment. The combination of comprehensive fetal phenotyping and advanced genomic analysis facilitates more accurate diagnosis,

improves recurrence-risk assessment, supports individualized genetic counseling, and contributes to informed prenatal and reproductive decision-making.

5. Conclusions

This study demonstrates the diagnostic contribution of prenatal WES in fetuses presenting with prenatally detected skeletal anomalies following non-diagnostic first-tier CMA. Pathogenic or likely pathogenic variants were identified in 15 of 24 fetuses (62.5%), while a phenotype-concordant molecular diagnosis was established in 11 cases (45.8%). These findings highlight the value of WES as a complementary diagnostic tool in the evaluation of suspected fetal skeletal disorders.

The marked locus heterogeneity and phenotypic overlap characteristic of fetal skeletal disorders highlight the diagnostic limitations of prenatal ultrasound alone and underscore the importance of integrating detailed fetal phenotyping with genomic analysis. Furthermore, the identification of incidental molecular findings and variants with uncertain phenotype relationships or variable expressivity emphasizes the need for careful variant interpretation and multidisciplinary genetic counseling to support parental decision-making and recurrence-risk assessment.

For cases without a phenotype-explanatory molecular finding, periodic reanalysis of exome sequencing data and consideration of complementary genomic approaches, such as whole-genome sequencing, may represent useful follow-up strategies as knowledge of disease-associated genes expands. Future prospective studies involving larger multicenter cohorts and systematic postmortem and postnatal phenotypic assessment are warranted to further refine genotype–phenotype correlations and optimize prenatal diagnostic approaches for fetal skeletal disorders.

Supplementary Materials: The following supporting information can be downloaded at: https://www.mdpi.com/article/10.3390/diagnostics16233911/s1, Figure S1. Case 4 (TD type 1): Multimodal imaging and genetic findings for the second case: (A–D) Serial prenatal ultrasound scans demonstrating shortening and bowing of the long bones, Figure S2. Case 18 (achondroplasia): Multimodal imaging findings and genetic profile for the third case (achondroplasia).

Author Contributions: Conceptualization M.P.M. and B.P.; methodology, M.P.M. and M.A.; formal analysis, M.A., I.M., T.J., S.V.P. and O.K.V.; investigation, M.P.M. and I.M.; writing—original draft preparation M.P.M., T.J. and I.M.; writing—review and editing, S.V.P., O.K.V. and B.P.; supervision, M.A. and B.P. All authors have read and agreed to the published version of the manuscript.

Funding: This research received no external funding.

Institutional Review Board Statement: The study was conducted in accordance with the Declaration of Helsinki and approved by the Ethics Committee of the University Clinical Center of Serbia (approval no. 705/22; date of approval: 4 August 2026).

Informed Consent Statement: Written informed consent was obtained from all parents of the fetuses included in the study.

Data Availability Statement: The data presented in this study are available on reasonable request from the corresponding author. The data are not publicly available due to privacy and ethical restrictions.

Acknowledgments: This work has been realized within the Center for Genetic Diagnostics of Rare Diseases, Institute of Molecular Genetics and Genetic Engineering.

Conflicts of Interest: The authors declare no conflicts of interest.

Abbreviations

The following abbreviations are used in this manuscript:

ACMG	American College of Medical Genetics and Genomics
CES	clinical exome sequencing
cfDNA	cell-free fetal DNA
CMA	chromosomal microarray analysis
CNVs	copy number variants
FGR	fetal growth restriction
IVF	in vitro fertilization
NMF-P	no molecular finding explaining the phenotype
P/LP	pathogenic/likely pathogenic
PGT	preimplantation genetic testing
PGR-U	phenotype–genotype relationship uncertain
SUA	single umbilical artery
SNVs	single-nucleotide variants
WES	whole exome sequencing

References

1. Mortier, G.R.; Cohn, D.H.; Cormier-Daire, V.; Hall, C.; Krakow, D.; Mundlos, S.; Nishimura, G.; Robertson, S.; Sangiorgi, L.; Savarirayan, R.; et al. Nosology and classification of genetic skeletal disorders: 2019 revision. *Am. J. Med. Genet. A* **2019**, *179*, 2393–2419. [CrossRef] [PubMed]
2. Savarirayan, R.; Rossiter, J.P.; Hoover-Fong, J.E.; Irving, M.; Bompadre, V.; Goldberg, M.J.; Bober, M.B.; Cho, T.J.; Kamps, S.E.; Mackenzie, W.G.; et al. Best practice guidelines regarding prenatal evaluation and delivery of patients with skeletal dysplasia. *Am. J. Obstet. Gynecol.* **2018**, *219*, 545–562. [CrossRef] [PubMed]
3. Schramm, T.; Mommsen, H. Fetal skeletal disorders. *Ultraschall Med.* **2018**, *39*, 610–634. [CrossRef] [PubMed]
4. Huang, Y.; Liu, C.; Ding, H.; Wang, Y.; Yu, L.; Guo, F.; Li, F.; Shi, X.; Zhang, Y.; Yin, A. Exome sequencing in fetuses with short long bones detected by ultrasonography: A retrospective cohort study. *Front. Genet.* **2023**, *14*, 1032346. [CrossRef] [PubMed]
5. Yeo, L.; Romero, R.J.; Gotsch, F.; Vaisbuch, E.; Pilu, G. Fetal skeletal anomalies. In *Sonography in Obstetrics and Gynecology: Principles & Practice*, 7th ed.; Fleischer, A.C., Toy, E.C., Lee, W., Manning, F.A., Romero, R.J., Eds.; McGraw-Hill Education: New York, NY, USA, 2015.
6. Gaudry, P.; Esvan, M.; Meynard, J.B.; Lebbar, A.; Choiset, A.; Lewin, F.; Tsatsaris, V.; Pannier, E.; Grange, G. Amniocentesis performed for karyotyping after identified ultrasonographic abnormalities: What to expect? *Fetal Diagn. Ther.* **2012**, *31*, 55–62. [CrossRef] [PubMed]
7. Liu, J.; Huang, L.; He, Z.; Lin, S.; Wang, Y.; Luo, Y. Clinical value of genetic analysis in prenatal diagnosis of short femur. *Mol. Genet. Genom. Med.* **2019**, *7*, e978. [CrossRef] [PubMed]
8. Tzadikevitch Geffen, K.; Singer, A.; Maya, I.; Sagi-Dain, L.; Khayat, M.; Ben-Shachar, S.; Daum, H.; Michaelson-Cohen, R.; Feingold-Zadok, M.; Sukenik Halevy, R. Chromosomal microarray should be performed for cases of fetal short long bones detected prenatally. *Arch. Gynecol. Obstet.* **2021**, *303*, 85–92. [CrossRef] [PubMed]
9. Vora, N.L.; Norton, M.E. Prenatal exome and genome sequencing for fetal structural abnormalities. *Am. J. Obstet. Gynecol.* **2023**, *228*, 140–149. Erratum in *Am. J. Obstet. Gynecol.* **2023**, *229*, 709. https://doi.org/10.1016/j.ajog.2023.09.017. [CrossRef] [PubMed]
10. Tang, H.; Zhang, Q.; Xiang, J.; Yin, L.; Wang, J.; Wang, T. Whole exome sequencing aids the diagnosis of fetal skeletal dysplasia. *Front. Genet.* **2021**, *12*, 599863. [CrossRef] [PubMed]
11. Landrum, M.J.; Lee, J.M.; Riley, G.R.; Jang, W.; Rubinstein, W.S.; Church, D.M.; Maglott, D.R. ClinVar: Public archive of relationships among sequence variation and human phenotype. *Nucleic Acids Res.* **2014**, *42*, D980–D985. [CrossRef] [PubMed]
12. Kopanos, C.; Tsiolkas, V.; Kouris, A.; Chapple, C.E.; Albarca Aguilera, M.; Meyer, R.; Massouras, A. VarSome: The human genomic variant search engine. *Bioinformatics* **2019**, *35*, 1978–1980. [CrossRef] [PubMed]
13. Richards, S.; Aziz, N.; Bale, S.; Bick, D.; Das, S.; Gastier-Foster, J.; Grody, W.W.; Hegde, M.; Lyon, E.; Spector, E.; et al. Standards and guidelines for the interpretation of sequence variants: A joint consensus recommendation of the American College of Medical Genetics and Genomics and the Association for Molecular Pathology. *Genet. Med.* **2015**, *17*, 405–424. [CrossRef] [PubMed]
14. Durkie, M.; Cassidy, E.J.; Berry, I.; Owens, M.; Turnbull, C.; Scott, R.H.; Taylor, R.W.; Deans, Z.C.; Ellard, S.; Baple, E.L.; et al. *ACGS Best Practice Guidelines for Variant Classification in Rare Disease 2024*; Royal Devon University Healthcare NHS Foundation Trust: Exeter, UK, 2024.
15. Wapner, R.J.; Martin, C.L.; Levy, B.; Ballif, B.C.; Eng, C.M.; Zachary, J.M.; Savage, M.; Platt, L.D.; Saltzman, D.; Grobman, W.A.; et al. Chromosomal microarray versus karyotyping for prenatal diagnosis. *N. Engl. J. Med.* **2012**, *367*, 2175–2184. [CrossRef] [PubMed]

16. Emms, A.; Castleman, J.; Allen, S.; Williams, D.; Kinning, E.; Kilby, M. Next generation sequencing after invasive prenatal testing in fetuses with congenital malformations: Prenatal or neonatal investigation. *Genes* **2022**, *13*, 1517. [CrossRef] [PubMed]
17. Yu, D.; Feng, D.; Qu, J.; Nie, L.; Liu, Q.; Gao, L.; An, W.; Liu, N.; Fang, Y. Application of trio-based whole-exome sequencing in fetal ultrasound anomalies: A single-center retrospective study of 454 cases. *Front. Genet.* **2025**, *16*, 1662801. [CrossRef] [PubMed]
18. Li, J.; Liang, S.; Miao, Y.; Du, X.; Han, M.; Zhao, W. Genetic analysis of 74 fetuses terminated for skeletal dysplasia and evaluation of diagnostic performance of whole exome sequencing. *Zhonghua Yi Xue Yi Chuan Xue Za Zhi* **2025**, *42*, 869–882. (In Chinese) [CrossRef] [PubMed]
19. Wang, L.; Zhang, Y.; Zheng, F.; Dong, H.; Zhu, X.; Jia, C.; Zhang, B. Genetic analysis of fetal skeletal dysplasia via whole exome sequencing and non-invasive prenatal diagnosis. *Ann. Med.* **2026**, *58*, 2606517. [CrossRef] [PubMed]
20. Striedner, Y.; Arbeithuber, B.; Moura, S.; Nowak, E.; Reinhardt, R.; Muresan, L.; Salazar, R.; Ebner, T.; Tiemann-Boege, I. Exploring the micro-mosaic landscape of FGFR3 mutations in the ageing male germline and their potential implications in meiotic differentiation. *Genes* **2024**, *15*, 191. [CrossRef] [PubMed]
21. Vasques, G.A.; Funari, M.F.A.; Ferreira, F.M.; Aza-Carmona, M.; Sentchordi-Montané, L.; Barraza-García, J.; Lerario, A.M.; Yamamoto, G.L.; Naslavsky, M.S.; Duarte, Y.A.O.; et al. IHH gene mutations causing short stature with nonspecific skeletal abnormalities and response to growth hormone therapy. *J. Clin. Endocrinol. Metab.* **2018**, *103*, 604–614. [CrossRef] [PubMed]
22. Zhou, Y.; Jiang, X.; Zhang, Y.; Zhang, Y.; Sun, F.; Ma, Y. Variant analysis and PGT-M of OTC gene in a Chinese family with ornithine carbamoyltransferase deficiency. *BMC Pregnancy Childbirth* **2024**, *24*, 491. [CrossRef] [PubMed]
23. Gong, W.Y.; Liu, F.N.; Yin, L.H.; Zhang, J. Novel mutations of COL4A5 identified in Chinese families with X-linked Alport syndrome and literature review. *Biomed Res. Int.* **2021**, *2021*, 6664973. [CrossRef] [PubMed]
24. Moresco, G.; Rondinone, O.; Mauri, A.; Costanza, J.; Santaniello, C.; Colapietro, P.; Micaglio, E.; Marfia, G.; Pesenti, C.; Grilli, F.; et al. Pitfalls of whole exome sequencing in undefined clinical conditions with a suspected genetic etiology. *Genes Genom.* **2023**, *45*, 637–655. [CrossRef] [PubMed]
25. Kimber, E.; Tajsharghi, H.; Kroksmark, A.K.; Oldfors, A.; Tulinius, M. Distal arthrogryposis: Clinical and muscle biopsy findings in a family with a novel MYH3 mutation. *Acta Paediatr.* **2012**, *101*, e87–e92. [CrossRef] [PubMed]
26. Monaghan, K.G.; Leach, N.T.; Pekarek, D.; Prasad, P.; Rose, N.C.; ACMG Professional Practice and Guidelines Committee. The use of fetal exome sequencing in prenatal diagnosis: A points to consider document of the American College of Medical Genetics and Genomics (ACMG). *Genet. Med.* **2020**, *22*, 675–680. [CrossRef] [PubMed]
27. Mei, Y.; Li, J.; Zhang, L.; Wei, X.; Xu, Q.; Shen, C.; Qin, Y.; Zhong, Q.; Li, Y. The clinical utility of whole-exome sequencing in the prenatal diagnosis of fetal skeletal dysplasia. *Int. J. Womens Health* **2026**, *18*, 576–580. [CrossRef] [PubMed]

Disclaimer/Publisher's Note: The statements, opinions and data contained in all publications are solely those of the individual author(s) and contributor(s) and not of MDPI and/or the editor(s). MDPI and/or the editor(s) disclaim responsibility for any injury to people or property resulting from any ideas, methods, instructions or products referred to in the content.